EUROPEAN SYNCHROTRON RADIATION FACILITY

INSTALLATION EUROPEENNE DE RAYONNEMENT SYNCHROTRON

ESRF

Experiment Report Form

The double page inside this form is to be filled in by all users or groups of users who have had access to beam time for measurements at the ESRF.

Once completed, the report should be submitted electronically to the User Office using the
Electronic Report Submission Application:

http://193.49.43.2:8080/smis/servlet/UserUtils?start

Reports supporting requests for additional beam time

Reports can now be submitted independently of new proposals – it is necessary simply to indicate the number of the report(s) supporting a new proposal on the proposal form.

The Review Committees reserve the right to reject new proposals from groups who have not reported on the use of beam time allocated previously.

Reports on experiments relating to long term projects

Proposers awarded beam time for a long term project are required to submit an interim report at the end of each year, irrespective of the number of shifts of beam time they have used.

Published papers

All users must give proper credit to ESRF staff members and proper mention to ESRF facilities which were essential for the results described in any ensuing publication. Further, they are obliged to send to the Joint ESRF/ ILL library the complete reference and the abstract of all papers appearing in print, and resulting from the use of the ESRF.

Should you wish to make more general comments on the experiment, please note them on the User Evaluation Form, and send both the Report and the Evaluation Form to the User Office.

Deadlines for submission of Experimental Reports

- 1st March for experiments carried out up until June of the previous year;
- 1st September for experiments carried out up until January of the same year.

Instructions for preparing your Report

- fill in a separate form for each project or series of measurements.
- type your report, in English.
- include the reference number of the proposal to which the report refers.
- make sure that the text, tables and figures fit into the space available.
- if your work is published or is in press, you may prefer to paste in the abstract, and add full reference details. If the abstract is in a language other than English, please include an English translation.

<table>
<tr>
<td rowspan="2">**ESRF**</td>
<td>**Experiment title:**

Solution structures of antibodies important in biotechnology and disease</td>
<td>**Experiment number**:
MX-1523</td>
</tr>
</table>

Beamline: BM29	**Date of experiment**: from: 28 Nov 2013 to: 29 Nov 2013	**Date of report**: 03/10/2014
Shifts: 3	**Local contact(s)**: Dr Adam Round	*Received at ESRF:*

Names and affiliations of applicants (* indicates experimentalists):

(1) Rayner, L. E.*, Hui, G. K.*, Gor, J., Heenan, R. K. Dalby, P. A. & Perkins S. J.* (UCL)

(2) Hilton, D.* , Perkins, S. J.* & Dalby, P. A. (UCL)

Abstract: Human IgG4 antibody shows therapeutically-useful properties compared to the IgG1, IgG2 and IgG3 subclasses. Thus IgG4 does not activate complement, and shows conformational variability. These properties are attributable to its hinge region, which is the shortest of the four IgG subclasses. Using high throughput scattering methods, we have studied the solution structure of wild-type IgG4(Ser222) and a hinge mutant IgG4(Pro222) in different buffers and temperatures, where the proline substitution suppresses the formation of half-antibody. Analytical ultracentrifugation showed that both IgG4 forms were principally monomeric with sedimentation coefficients $s^0_{20,w}$ of 6.6-6.8 S. A monomer-dimer equilibrium was observed in heavy water buffer at low temperature. Scattering showed that the X-ray radius of gyration R_G was unchanged with concentration in 50-250 mM NaCl buffers, while the neutron R_G values showed a concentration-dependent increase as the temperature decreased in heavy water buffers. The distance distribution curves *P(r)* revealed two peaks, *M1* and *M2* that shifted below 2 mg/ml to indicate concentration-dependent IgG4 structures, in addition to IgG4 dimer formation at high concentration in heavy water. Constrained X-ray and neutron scattering modelling revealed asymmetric solution structures for IgG4(Ser222) with extended hinge structures. The IgG4(Pro222) structure was similar. Both IgG4 structures showed that their Fab regions were positioned close enough to the Fc region to restrict C1q binding. Our new molecular models for IgG4 explain its inability to activate complement, and clarifies aspects of its stability and function for therapeutic applications.

(2) Report: Biophysical analysis of aggregation-prone states of antibody Fab antigen-binding fragment. Hilton, D.*, Perkins, S. J.* & Dalby, P. A. (2014)

Introduction: Product losses through the formation of aggregates are still a major problem at each stage of a therapeutic protein's life, from its effects on expression within the cell through to the shelf life of the packaged product. These aggregates are typically undesirable since they are a manifestation of the target molecules physical instability and result in both reduced activity and increased immunogenic potential. The aggregation kinetics of a therapeutic Fab have been characterised by us in detail over a wide range of conditions, and aggregation appears to be promoted by a near-native intermediate state in solution. This study investigated the Fab over the same range of conditions, at time-zero prior to aggregation, to identify structural changes in the native protein consistent with an intermediate state. SAXS measurements were performed upon the Fab fragment at a variety of solvent ionic strengths and pHs, and a shift in the radius of gyration was observed predominantly in the more aggregation prone conditions. The shift was consistent

with a near-native intermediate state that is strongly pH dependent. The high-throughput capabilities of the BM29 Bio-SAXS beamline enabled 20 solution environments to be examined (5 pH x 4 ionic strengths), with each condition measured in triplicate.

Radius of gyration and P(r) analyses: Scattering curves for the 60 samples, each containing 1mg/ml of Fab', were collected and analysed using *AutoRg* to estimate the radius of gyration from the Guinier regions. These values were in good agreement with those calculated from integration of the real space distribution functions, P(r), for each of the measurements. Each P(r) plot was characterised by a smooth peak with a single maxima, M, at 2.85 ± 0.03nm and a characteristic length, L, of 9.58 ± 0.32. The deviations in L present are likely to result from the formation of low levels of aggregate within solution. By plotting the protein size as a function of both pH and ionic strength (Fig. 1) it can be seen that an increasingly acidic environment causes a gradual increase in the measured average radius of gyration of the molecule. This could be explained by relaxation of regions within the molecules structure or subtle changes in conformation, for instance bending at hinges between the domains. The effects of ionic strength are less pronounced except in the case of a highly acidic, low ionic strength system for which the molecules size is much lower than might be expected.
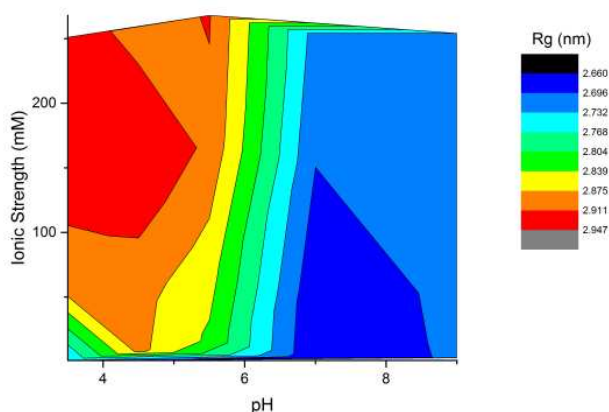
Figure 1: Contour plot illustrating changes in the proteins radius of gyration as function of solvent pH and ionic strength. Rg values were calculated from integrating p(r) curves for each of the measurements performed, and averaging triplicate data for each condition examined.

Relating protein conformation to aggregation propensity: To identify the protein's susceptibility to aggregate, forced degradation studies were performed with 1 mg/ml Fab' in each of 20 solution environments. Kinetic parameters for each of the conditions were subsequently derived using size exclusion chromatography. A plot of aggregation rate, in the form of monomer half-life, against the protein's radius of gyration at time zero reveals 3 distinct clusters of data (Fig. 2). Whilst one such cluster exhibits relative invariance in Rg versus aggregation half-life (mechanism 2), an apparent link between the variables is evident in the other two data clusters (mechanism 1). It is thought that this difference could be attributed competing aggregation mechanisms depending upon the solvent conditions selected. Quantification of the net protein-protein interactions within the system suggest that the aggregation propensity for points following mechanism 2 is colloidally controlled, whilst mechanism 1 is subject to greater conformational control. In addition, mechanism 2 conditions are mostly pH5.5 at which point the strength of salt bridges is at a maximum. We now hypothesise that aggregation is promoted by acidic conditions through increased dynamic and partial unfolding of the structure, while it is also suppressed under conditions which optimise the stability of salt bridges.
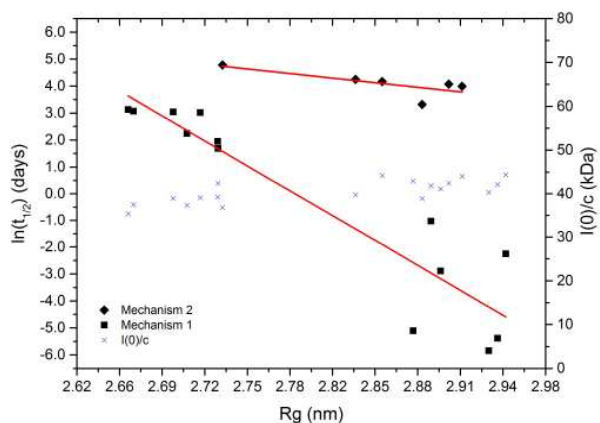
Figure 2: Correlation between radius of gyration and sample aggregation rate, showing apparent clustering of data points. I(0)/c also included to show independence of correlation from presence of low aggregate levels within the sample.

Conclusion: A clear link between the initial radius of gyration of a protein and its solvent composition has been identified, particularly its pH and ionic strength. It is well known that both of these variables strongly influence a proteins propensity to aggregate but the mechanism behind this remains only partially understood. SAXS is providing crucial insights into how changes in the protein's structure might be involved in this process.